SI/Note DL/69-18
9-12.1969

BEAM SCRAPERS IN THE PSB

C. Bovet

1. Injection region
   - 1.1 Curved septum
   - 1.2 Straight septum
   - 1.3 Protection of the septum
2. Shadow target
   - 2.1 Temperature increase of the stopping medium
   - 2.2 Maximum proton flux
3. Protection of PSB components
   - 3.1 Vacuum chamber
   - 3.2 Special components

Introduction

One aim is to protect the machine components against radiation damage produced when a high flux of particles is concentrated on a small surface during a time shorter than 1 ms (see ref.1). The second aim is to prevent even smaller proton fluxes from hitting some more sensitive components (pick-up electrodes, kickers etc.). These tasks are achieved by shadow targets and static diaphragms called scrapers.

But there will be no consideration on how to cut the tail of the betatron amplitude distribution for cleaning the beam as proposed by Teng[2] for NAL. This sort of beam shaving will be done with the moving target units[3].

1. Inflector region

1.1 Curved septum

In order to discuss the loss of particles on the inflector let us approach the question by considering the three cases of Fig. 1. Cases a and b are self-explanatory, in case c the function f(x) corresponds to those trajectories of beam (2) which are tangent to the septum circle with radius R = ρ.

Fig. 2 gives the cut produced in the phase plane by a curved target for different values of the curvature radius R. Looking in the same direction Maschke[4] calculated once an effective septum thickness. But we shall consider the question more in detail.

Let us assume a long septum inflector with a bending radius $\rho \cong 30$ m.

Fig. 3 shows the phase plane diagram for multiturn injection of a Linac beam with $\epsilon_o = 10\ \pi$ mrad mm, matched to $\beta_H = 2$ m and centred 5 mm away from the septum. The septum thickness is 1 mm, the phase plane corresponds to the downstream end of the septum as for the examples in Fig. 1, the end of the septum is parallel to the injector beam and to the closed orbit.

Under these circumstances, with a curvature radius $R = \rho = 30$ m the dashed area is progressively cut from the incoming beam along the whole septum length.

In practice most of this loss may be avoided either by choosing a double curvature radius of the septum (see the dashed lines corresponding to R = 60 m in Fig. 3), or by adjusting the septum angle to + 3 mrad (which is equivalent to translating both Linac and PSB beams downwards by 3 cm in Fig. 3). The first method is the best one at least for the downstream part of the septum.

Let us consider first the particles lost on the concave side of the septum (i.e. Linac beam). Different points of that surface marked by crosses in Fig. 4a produce the corresponding cuts in the phase plane of Fig. 5b. In the case considered here no loss occurs upstream the point $\ell = 0.6$ m. It is therefore evident that a target placed upstream the septum cannot be used to avoid hitting the septum under normal conditions. The only necessary thing is a special target protecting the upstream end at each septum for the cases where the beam is not correctly adjusted.

On the convex side passes the PSB circulating beam. With a nominal emittance and ± 1 mrad closed orbit one has $\hat{x}' = \pm 6$ mrad. Particles with $x' = -6$ mrad will graze the septum at $\ell = .36$ m. Upstream from this point it will be possible either to increase the septum thickness (as suggested by T.R. Sherwood) or to protect it by an appropriate slim target.

In Fig. 4a several points of that surface are shown with black circles.

Corresponding cuts in the phase plane are shown in Fig. 5a. The area occupied by the PSB beam is not well defined since it will depend completely on the parameters of the multiturn injection, it is therefore marked by a dashed line. Many more particles are likely to be lost upstream the tangent point ($\ell = 0.36$ m) than downstream so that a shadow target will be useful.

1.2 Straight septum

With a magnetic version of the PSB inflector another set of parameters is feasible[5] :

- bending radius ρ = 12 m
- septum length ℓ = 0.8 m
- variable septum thickness (concave for the Linac beam, straight for the PSB-beam)
- angle of the straight part : - 6 mrad.

The layout of this type of septum is shown on Fig. 4b. The septum is straight on the PSB-beam side but three different shapes are considered on the Linac beam side :

i) A septum curvature equal to the beam bending radius (R = ρ = 12 m) is excluded as seen from Fig. 6, phase plane diagram.

ii) A curvature R = 20 m would be seen from the beam trajectory as a target with R' = 30 m since $\frac{1}{R'} = \frac{1}{\rho} - \frac{1}{R}$. This shape is marked by crosses on Fig. 4b and corresponds to an effective septum thickness 0.5 mm bigger than the mechanical thickness (see Fig. 6). The particles get lost along the distance $0.2 < \ell < 0.7$ m, but there is no loss in the downstream part (20 cm) as seen from Fig. 7c.

iii) A constant thickness of the septum would lead to the straight shape marked by open circles on Fig. 4b. The corresponding cut in the phase plane is shown on Fig. 6 (R = ∞) and the particles would get lost mainly at $0.1 < \ell < 0.3$ m as seen from Fig. 7b.

On the PSB-beam side every three cases discussed above are ideal (see Fig. 6) and the particles are progressively lost on the septum length as shown on Fig. 7a.

1.3 Protection of the septum

On the Linac beam side no loss can be cured by using a shadow target as shown on Fig. 5 and Fig. 7, even in the case of a short septum (ℓ = 0.8 m). On the other hand shaving the beam $\lambda/2$ upstream is not compatible with the necessary betatron matching.

A shadow target is nevertheless useful for the protection of the upstream end of the septum in case of a bad adjustment of the injection parameters.

On the PSB-beam side the septum will not suffer from the beam because the angle of incidence is very small (see § 2.1) but a shadow target must be foreseen to cover the gap from the inflector septum (innermost radial position) to the vacuum chamber aperture. This shadow target might well be composed of two or three parts to fit the particular layout of the elements in 1L1.

Downstream the injection point there is no obvious azimuth where a big loss is foreseen to occur during multiturn injection.

2. Shadow target

2.1 Temperature increase of the stopping medium

A concentration of particles such that a flux of 10^{13} - 10^{14} p/cm^2 hits a surface perpendicular to the beam, will be a great danger for the component, as it was shown in Ref. 1. The angle of incidence α of the beam onto the target surface is very sensitive a parameter as far as the local heat deposit inside the stopping medium is concerned. The maximum heat deposit occurs when the particle stops in the medium. But due to the stochasticity of energy loss and multiple scattering, a monokinetic zero-emittance beam will stop with an ellipsoidal distribution inside the medium, as shown in Fig. 8a. The small axis a of the ellipse is due to the "range-straggling", b is the lateral displacement due to the scattering. At 50 MeV one has grossly for any material[6)]

$$a \cong 0.015 \text{ range}$$

$$b \cong 0.05 \text{ range}$$

The local temperature increase in the medium is then (see also Fig. 8b and 8c).

$$\frac{\Delta T(90^o)}{\Delta T(\alpha)} = \sqrt{1 + \left(\frac{b}{a \tan\alpha}\right)^2} \qquad (1)$$

Nevertheless even for very small α, there is an upper limit to the ratio $\Delta T(90^o)/\Delta T(\alpha)$ due to the finite ratio

$$\left(\frac{dE}{dx}\right)_{max} / \frac{dE}{dx}\,(50 \text{ MeV}) \approx 30 \quad \text{(see Ref. 6)}$$

2.2 Maximum proton flux

Two different situations may produce a maximum flux of protons :

i) The whole Linac beam is used for one revolution studies

$$\phi_{max}\left[p/cm^2\right] = 100\,\frac{I_o\,\Delta t}{e\pi\epsilon_o\sqrt{\beta_x\beta_z}}\,, \text{ (see Appendix)} \qquad (2)$$

where I_o, ϵ_o and Δt are Linac parameters used in Ref. 9) and $\beta_{x,z}$ are the PSB β-functions at the azimuth of the loss.

With the following values

$$I_o = 100 \text{ mA}$$
$$\Delta t = 100\ \mu s$$
$$\epsilon_o = 10\ \pi \text{ mm mrad}$$
$$\beta_x \equiv \beta_z = 5 \text{ m},.$$

one gets $\phi_{max} = 4.10^{13}$ p/cm^2.

ii) The circulating beam of one ring is progressively scraped of on a single element, for instance with a spiralling beam at small $\dot{B}$ one could have the total beam hitting a very small surface $\Delta s = 0.1\ cm^2$, so that

$$\phi_{max} = \frac{I_o\ \Delta t}{4e\ \Delta s} = 16.10^{13}\ p/cm^2 \qquad (3)$$

In both cases the consequences are tolerable provided the angle of incidence on the target element is small (as shown in § 2.1). In the first situation considered the upstream end of the inflector septum (septa) is the most dangerous point, in the second situation the upstream end of the ejection septum plays the same part.

3. Protection of PSB components

As far as heat damage is concerned a shadow target scheme is effective because the main purpose is to scatter out the particles. If one aims at reducing radiation damage or ionization of the residual gas by scattered particles, or secondary emission, the build up factor is more than one and the angular distribution of the effect is peaked in the beam direction, so that no effective shadow can be projected by a diaphragm located upstream.

But for particles drifting at a rate $\frac{\Delta y}{trev}$ a scraper placed downstream the component, with a semi-aperture $a_{scraper} = a_{component} - \Delta y$, will be an effective protection.

3.1 Vacuum chamber

The corrugated vacuum chamber must be protected against the high flux of a spiralling beam. This may be achieved by putting many scrapers around the machine.

Due to the β-functions, location ③ (and the symmetrical one) is the only dangerous point for the corrugated chamber. Let us put there (i.e. in the vacuum connection flange[8]) a beam scraper with an aperture smaller than the vacuum chamber by 2 mm in radius, and with a special radial limitation shown as curve ③ of Fig. 9 a.

On 14B2, 15B1 and 1B1 an extra large radial aperture is necessary for injection and ejection purposes. At these three points the scrapers will be designed without the special radial limitation, but still with a 2 mm reduction in radius all around the aperture. Corresponding scrapers and beam shapes are shown on Fig. 10.

3.2 Special components

- Pick up electrodes : it is seen from Fig. 9b that the beam cross section at locations (8) and (9) will not exceed a circle with 60 mm radius what gives a sufficient clearance.

- RF Cavity : the inner radius of this component is 58 mm what gives just 2 mm clearance at location (2) (see Fig. 9a). Since the phase advance from the nearest scraper to the cavity is $\Delta\varphi = \pm 18^{o}$ and $1 - \cos \Delta\varphi = 0.05$, no closed orbit with an amplitude $a \leq 35$ mm might hit the cavity.

- Kickers in long straight sections have the following aperture : E-K (115 x 70), I-KF (120 x 70), I-KS (Ceramic tube inner diameter = 120 mm), so that they will all be protected by the scrapers.

- Components in L4 : multiturn kickers I-KS located in 16L4 and 1L4 are not well protected by the scrapers there (see Fig. 10b, curves (6) to (10)) but do not forget that the closed orbit will be especially well corrected in this region.

Acknowledgements

During the 51st parameter meeting this note benefitted of discussion with Y. Baconnier, G. Brianti, G. Guignard, H. Koziol, P. Lefèvre, J.H.B. Madsen, K.H. Reich, C.E. Rufer, T.R. Sherwood.

Distribution : List MPS-SI/2

References

1. C. Bovet, Heat Deposit by a Proton Beam, SI/Note DL/69-11.

2. L.C. Teng, Design Concepts for the Beam Scraper System of the Main Ring, NAL - FN 196.

3. H. Koziol, Targets for the PSB, Note in preparation.

4. A. Maschke, Effective Width of Septa, NAL - FN 96.

5. T.R. Sherwood, Private Communication.

6. Joseph F. Janni, Calculation of Energy Loss, Range, Pathlength, Straggling, Multiple Scattering, and the probability of Inelastic Nuclear Collisions for 0.1 - to 1000 MeV protons, AFWL-TR-65-150 (1966).

7. C. Bovet, Apertures in the Booster, SI/Note DL/69-20.

8. C.E. Rufer, Private Communication.

9. C. Bovet, Filling the PSB with linac Beam, SI/Note DL/69-15.

APPENDIX

Let us assume a Linac current/emittance function given by :

$$I = Io\ (1-e^{-\epsilon/\epsilon_o}) \ . \qquad (A.1)$$

The density is :

$$\frac{dI}{d\epsilon} = \frac{Io}{\epsilon_o}\ (e^{-\epsilon/\epsilon_o}) \quad , \qquad (A.2)$$

or in term of a normalized distribution :

$$\frac{dn}{d\epsilon}\ d\epsilon = \frac{1}{\epsilon_o}\ e^{-\epsilon/\epsilon_o}\ d\epsilon \ . \qquad (A.3)$$

Expressed in the physical phase plane coordinate (x,x') by Courant and Snyder invariant the emittance is :

$$\epsilon = \gamma x^2 + 2\alpha x x' + \beta x'^2 \ . \qquad (A.4)$$

We now change to normalized coordinates (ξ, η) in order to separate variables and connect to the betatron phase advance ψ :

$$\begin{pmatrix}\xi\\ \eta\end{pmatrix} = \begin{pmatrix}1/\sqrt{\beta} & 0\\ \alpha/\sqrt{\beta} & \sqrt{\beta}\end{pmatrix}\begin{pmatrix}x\\ x'\end{pmatrix} \ . \qquad (A.5)$$

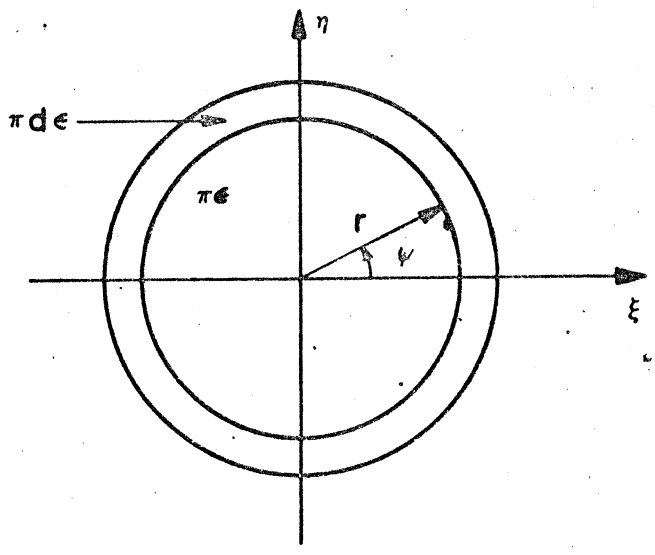

Transforming (A.4) by (A.5) gives :

$$\epsilon = \xi^2 + \eta^2 = r^2 \ , \tag{A.6}$$

and one has the circular emittance of the upper figure with ψ being the betatron phase advance. An equiprobability of ψ (i.e. equidensity of particles on a circle of the normalized phase plane) allows us to define the phase plane density $\rho(\xi, \eta)$ since :

$$\frac{dn}{d\epsilon} d\epsilon = \frac{dn}{dS} dS = \frac{1}{\epsilon_o} e^{-r^2/\epsilon_o} 2rdr \ , \tag{A.7}$$

changing to (ξ, η) by using $dS = 2\pi rdr = d\xi d\eta$, gives :

$$\frac{dn}{dS} dS = \rho(\xi, \eta) dS = \frac{1}{\pi\epsilon_o} e^{-\frac{1}{\epsilon_o}(\xi^2 + \eta^2)} d\xi d\eta \ . \tag{A.8}$$

Now integrating over $d\eta$ will give the profile $\frac{dn}{d\xi}$,

$$\frac{dn}{d\xi} d\xi = \int_{-\infty}^{\infty} \rho(\xi, \eta)\, d\xi\, d\eta = \frac{1}{\sqrt{\pi\epsilon_o}} e^{-\frac{1}{\epsilon_o}\xi^2} d\xi \ , \tag{A.9}$$

which turns out to be in the physical coordinates (x, x')

$$\frac{dn}{dx} dx = \frac{1}{\sqrt{\pi\beta_x\epsilon_o}} e^{-\frac{1}{\epsilon_o\beta_x}x^2} dx \ . \tag{A.10}$$

The linear maximum current density of the Linac beam is then :

$$\left(\frac{dI}{dx}\right)_{max} = \frac{Io}{\sqrt{\pi\beta_x\epsilon_o}} \ , \tag{A.11}$$

and the maximum current density in the cross section is :

$$\left(\frac{dI}{dxdz}\right)_{max} = \frac{Io}{\pi\epsilon_o\sqrt{\beta_x\beta_z}} \ . \tag{A.12}$$

a. Short target

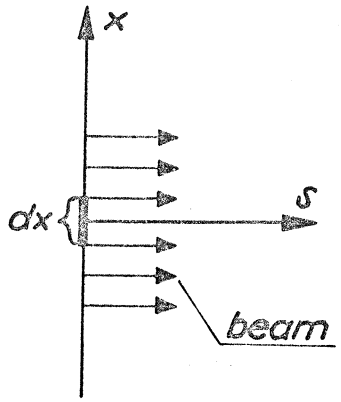

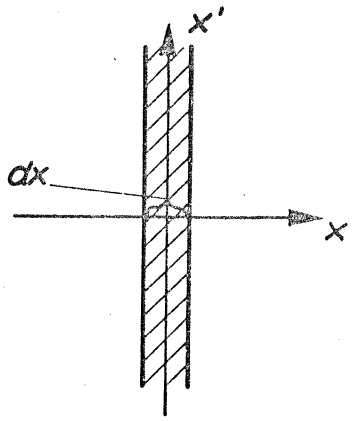

b. Long target

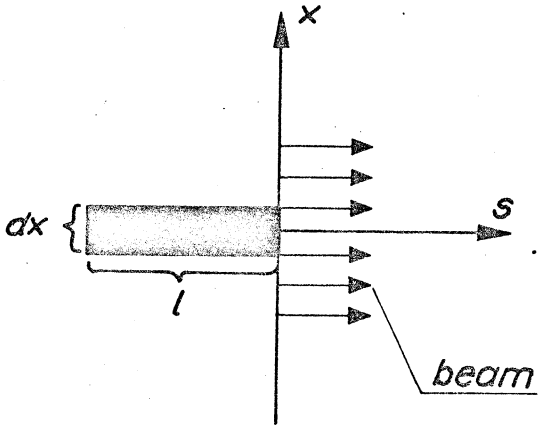

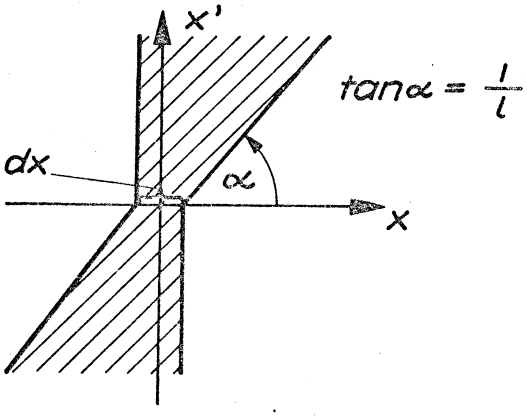

c. PSB inflector

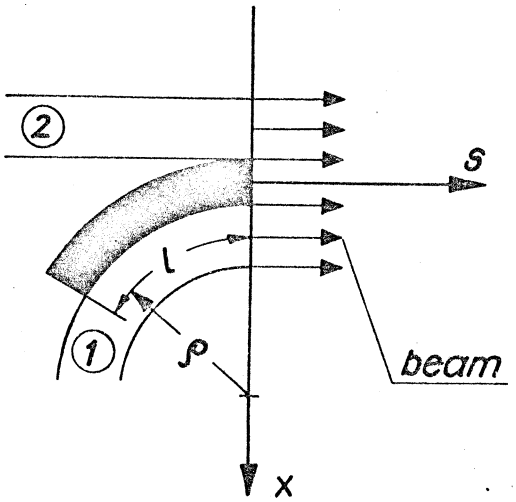

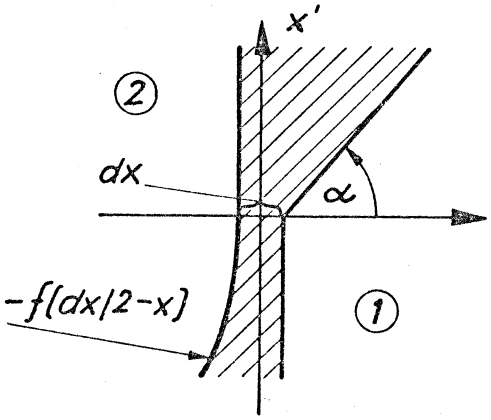

$f(x) = \sqrt{x^2 + 2Rx}\,/R$

$R = \rho$

Fig. 1

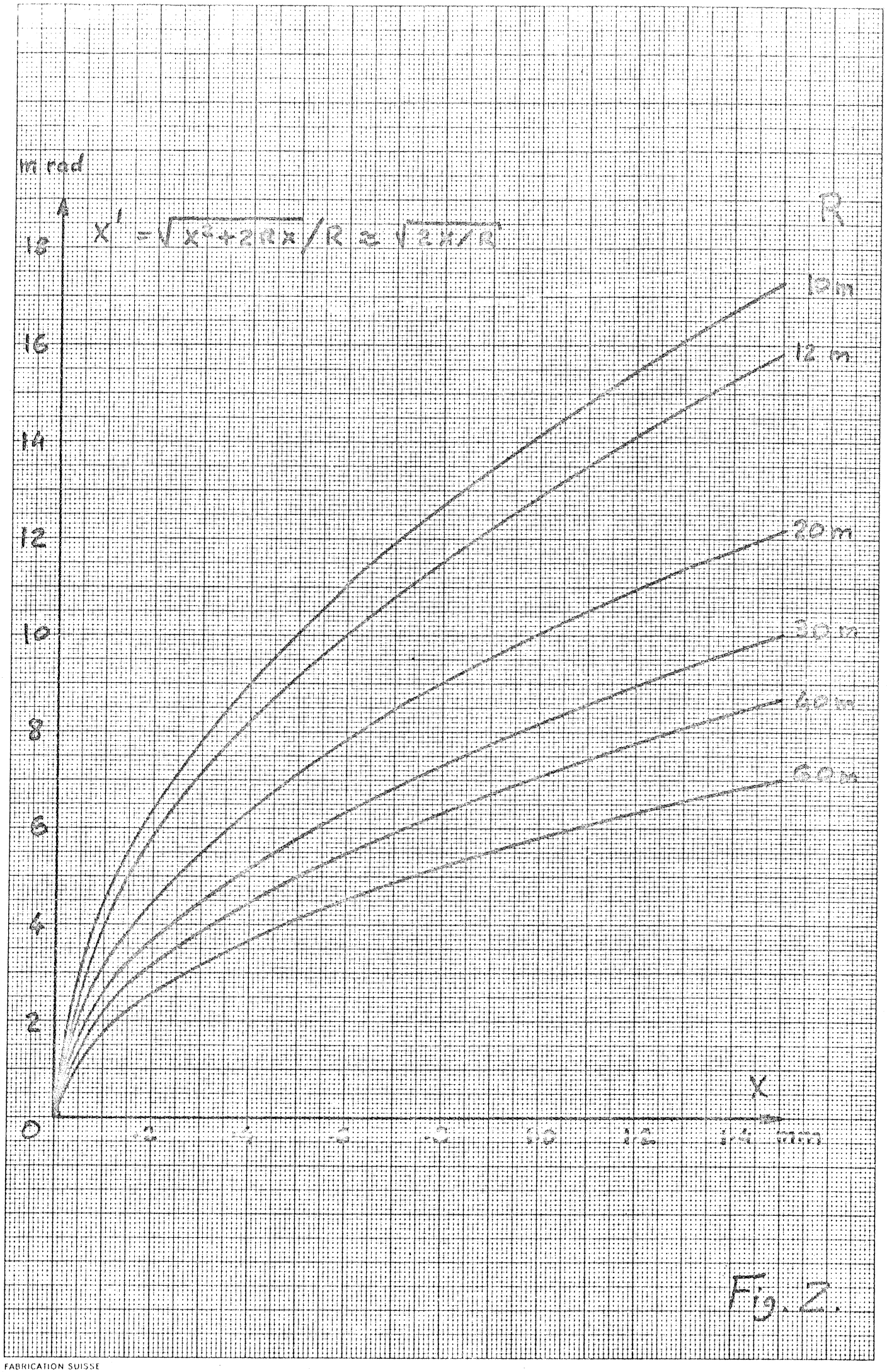

Fig. 2.

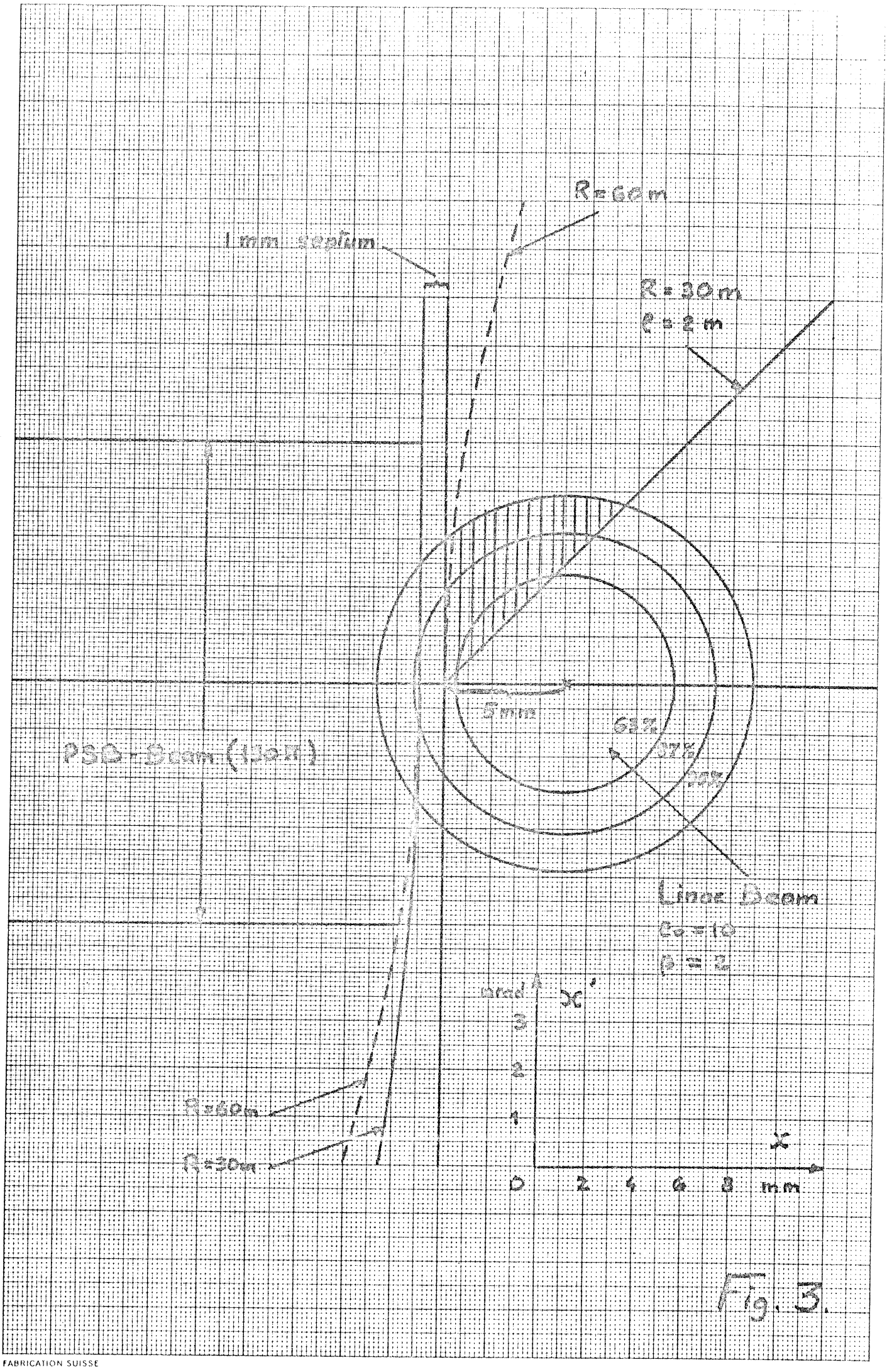

Fig. 5.

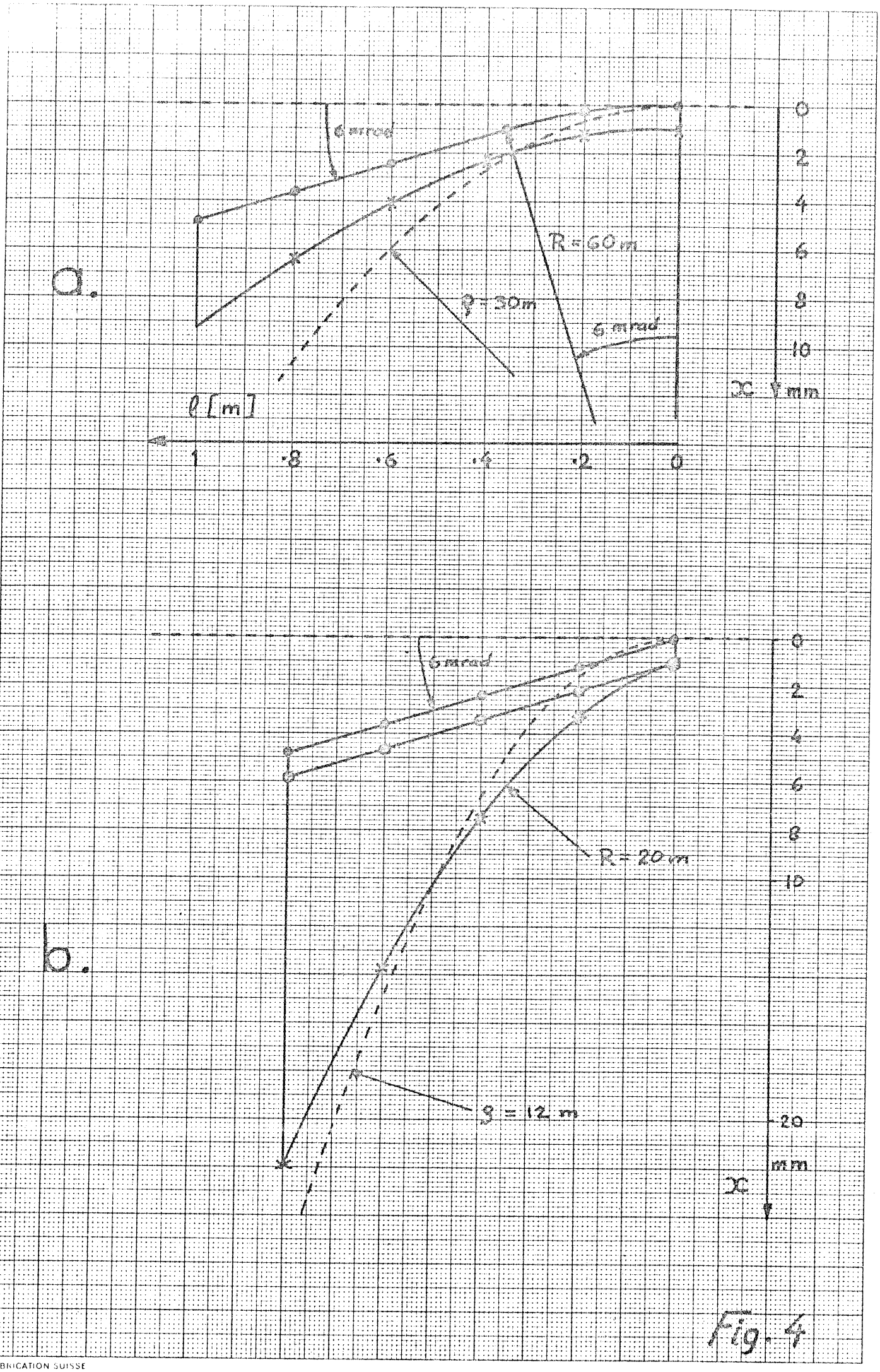

Fig. 4

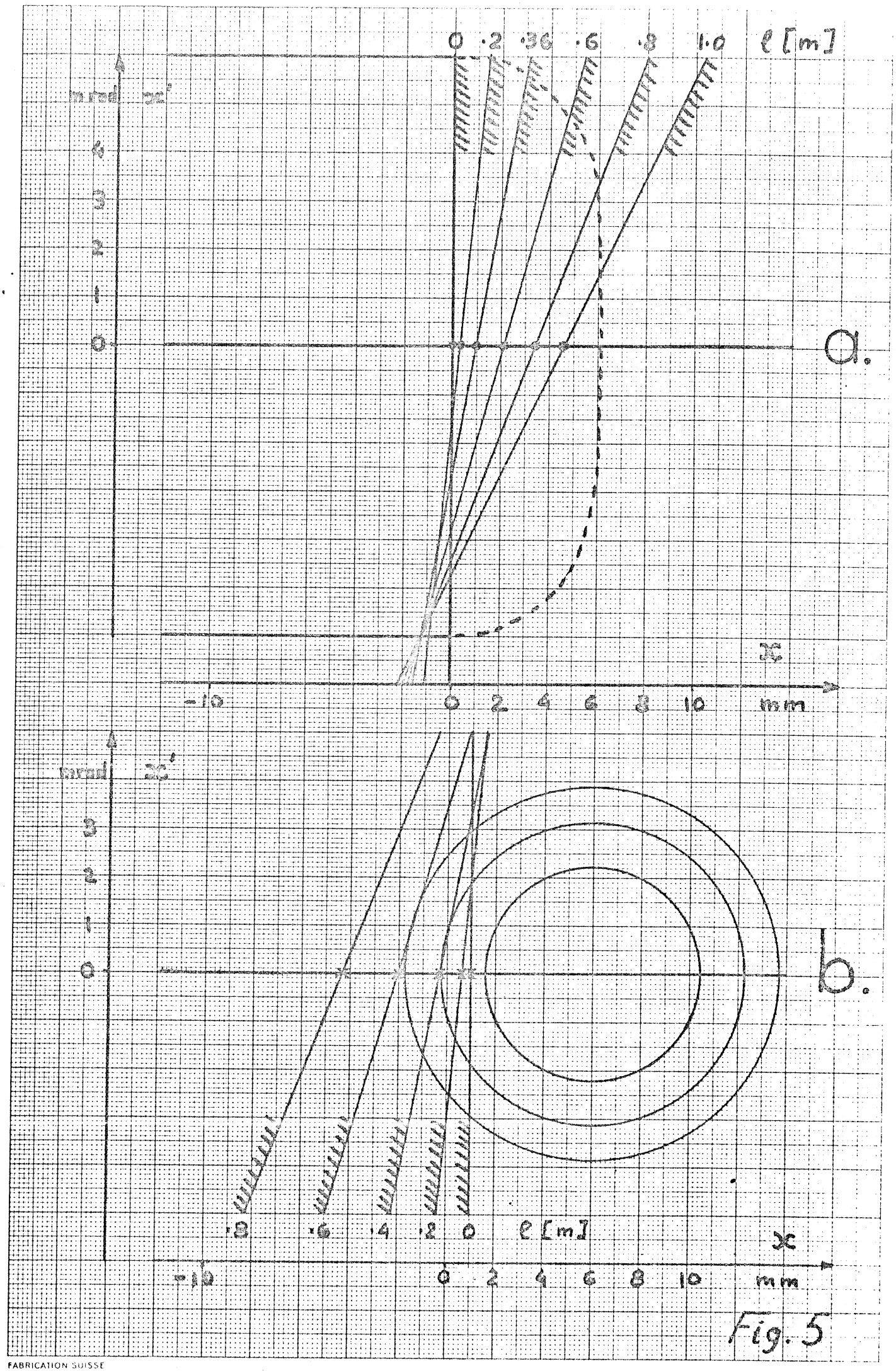

Fig. 5

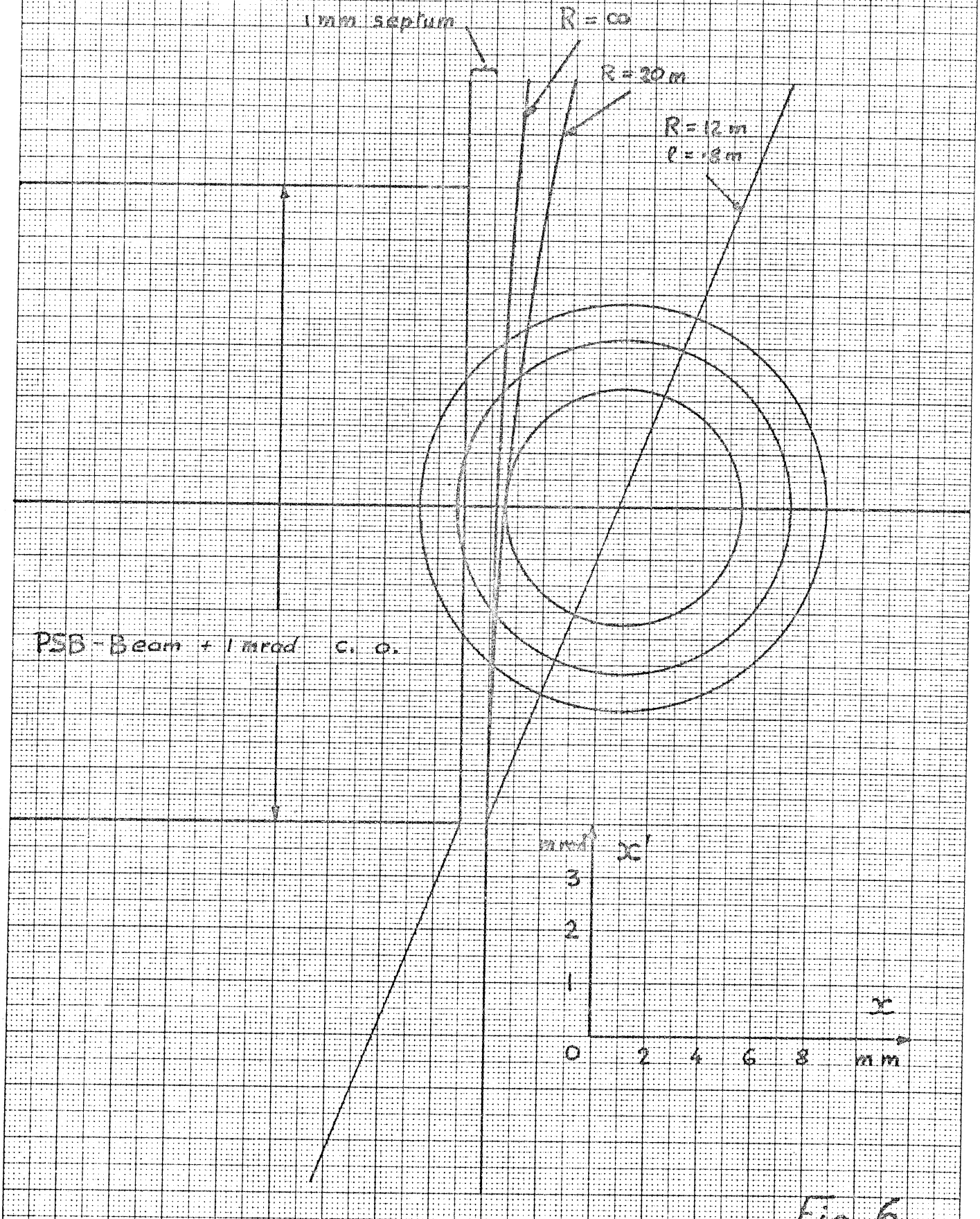

Fig. 6

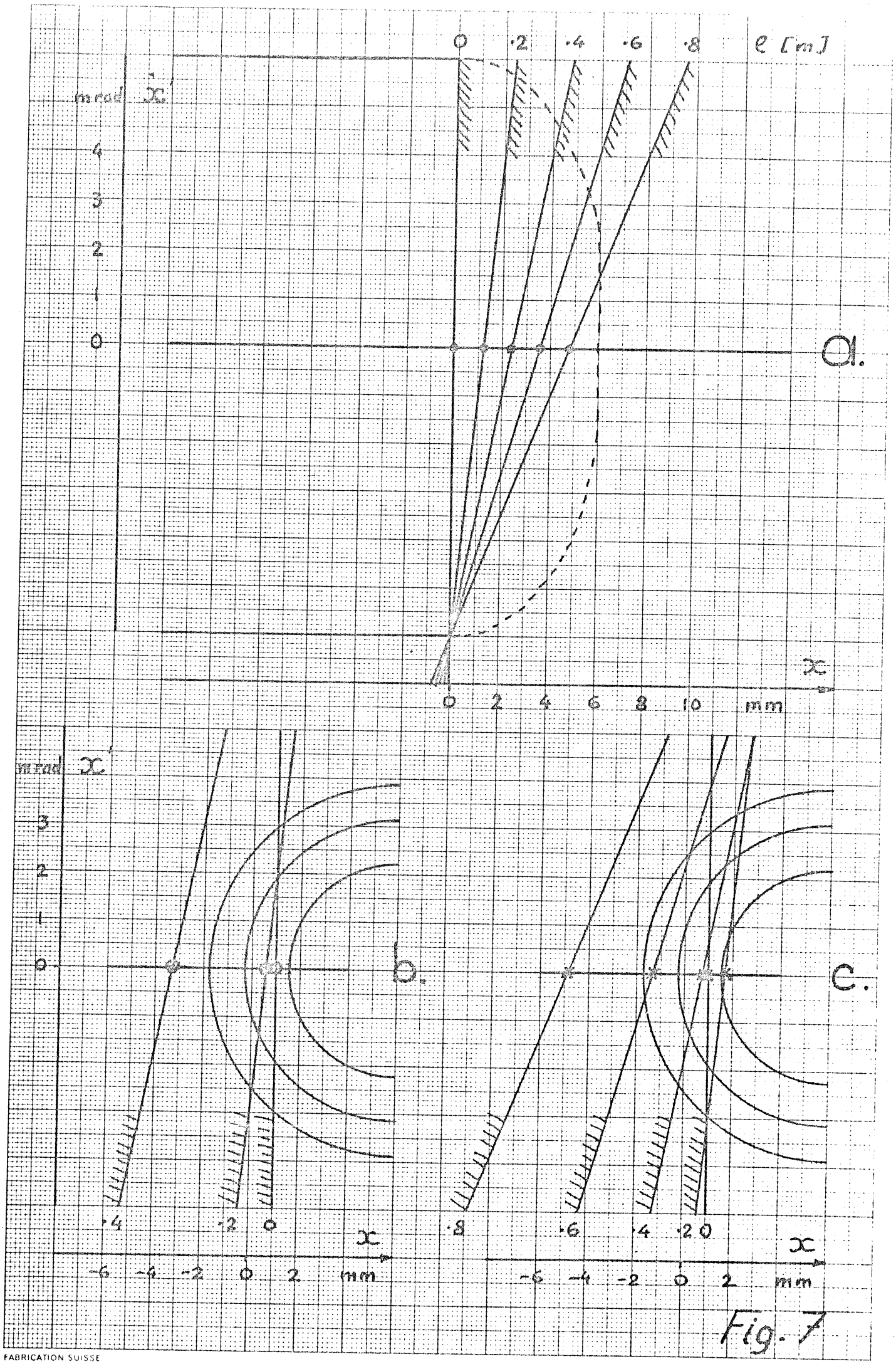

Fig. 7

FABRICATION SUISSE

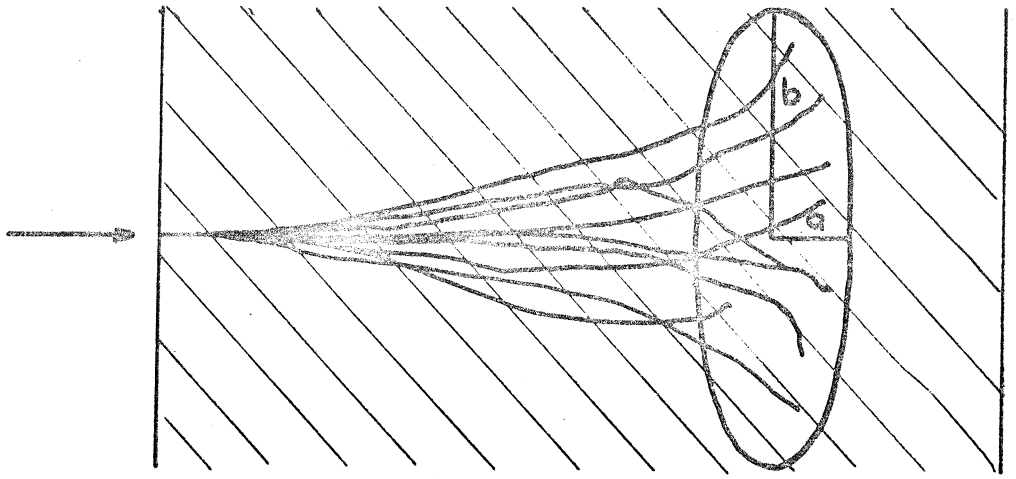

a.

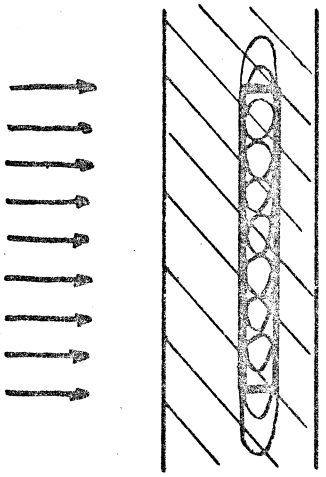

b.

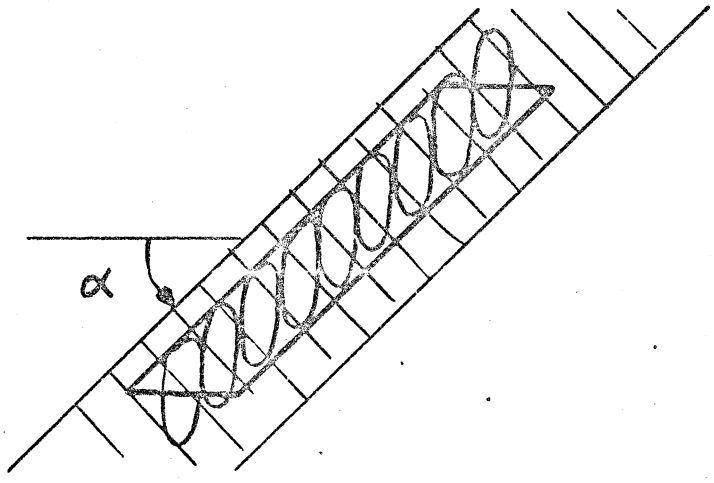

c.

Fig. 8

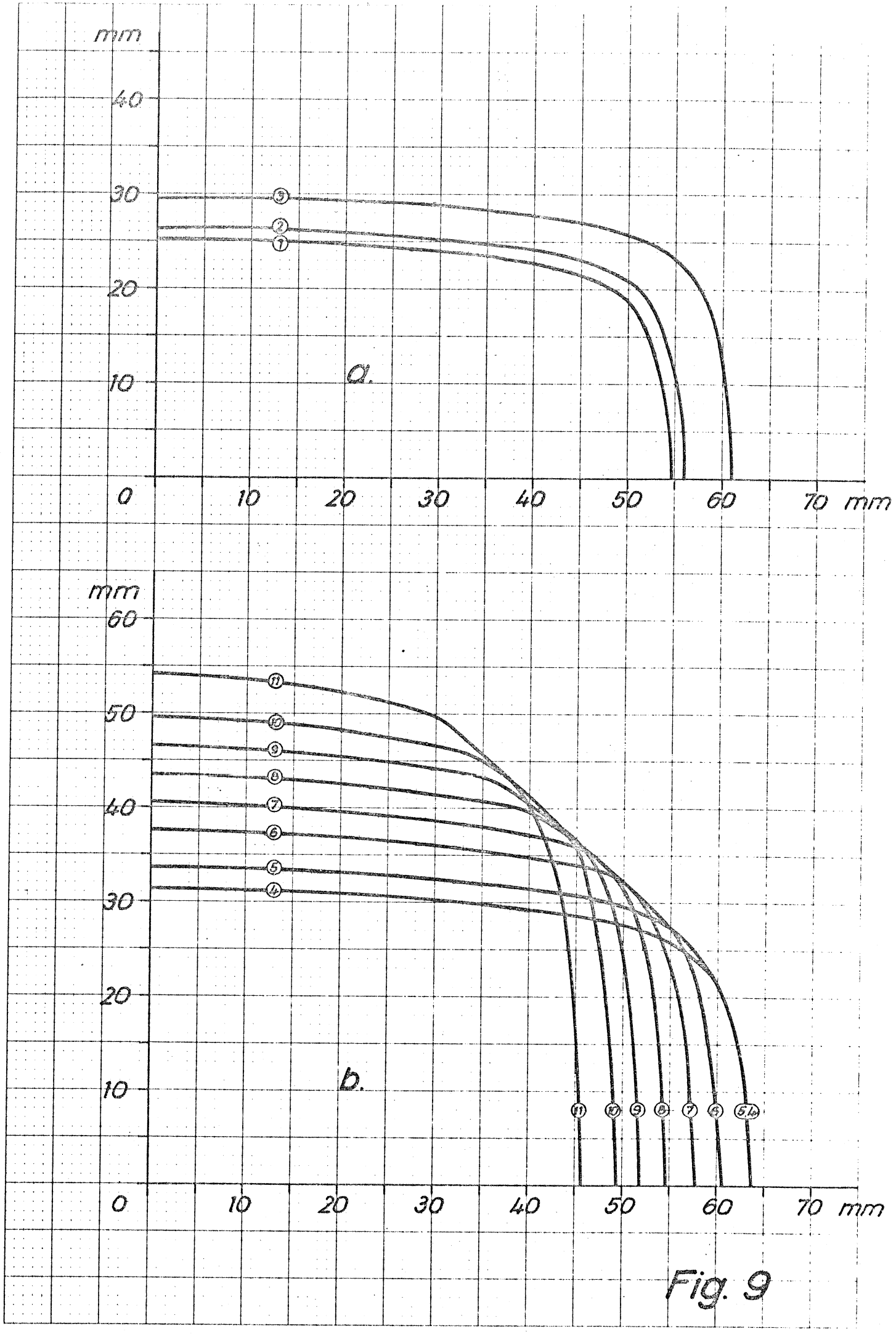
mm
40
30
20
10
0
10
20
30
40
50
60
70 mm
3
2
1
a.
mm
60
50
40
30
20
10
0
10
20
30
40
50
60
70 mm
11
10
9
8
7
6
5
4
b.

Fig. 9

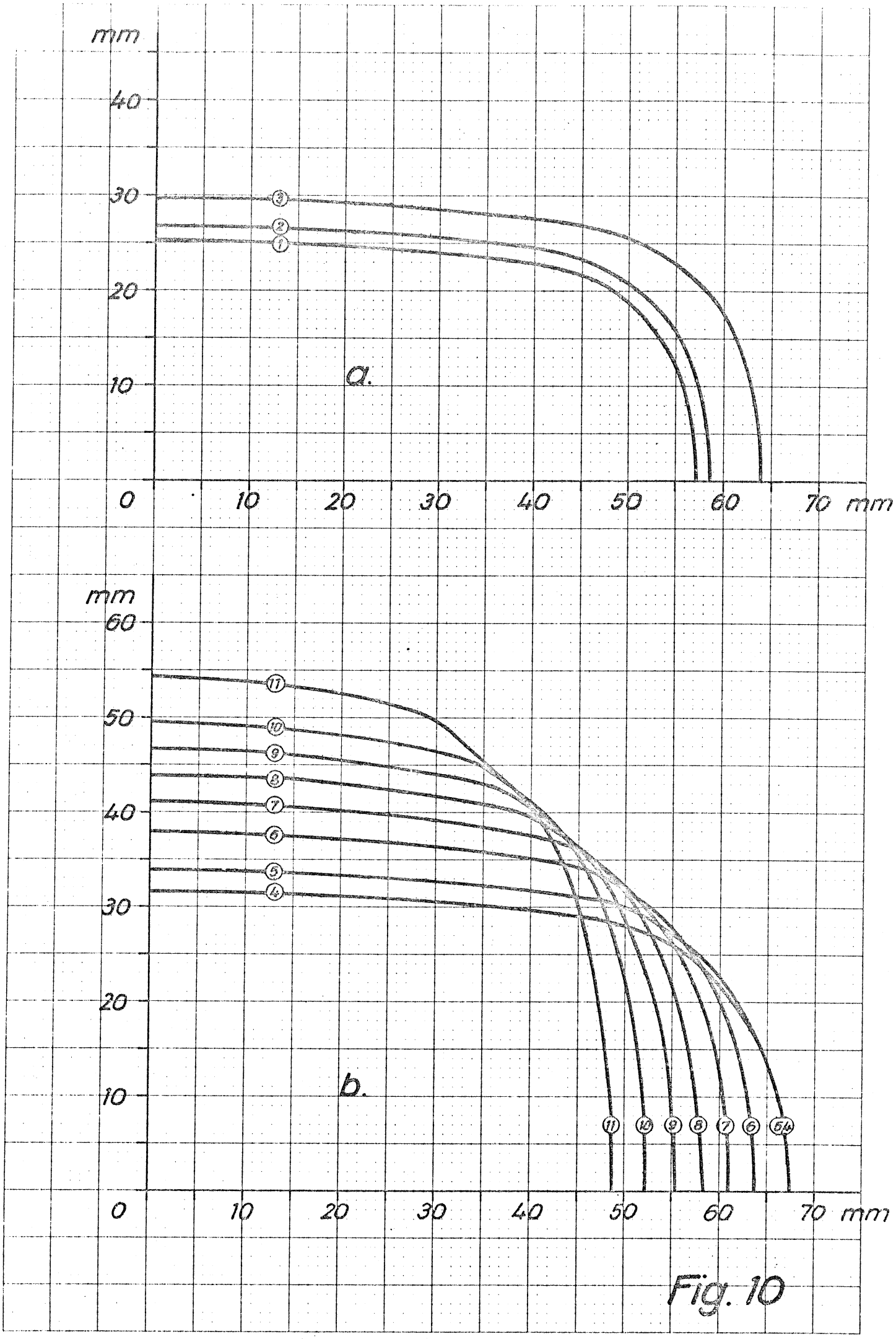
mm
40
30
20
10
3
2
1
a.
0
10
20
30
40
50
60
70 mm
mm
60
50
40
30
20
10
11
10
9
8
7
6
5
4
b.
11
10
9
8
7
6
5 4
0
10
20
30
40
50
60
70 mm

Fig. 10